Research on Parkinson's Disease Detection Based on Deep Residual Shrinkage Network

Mingze Yu *

Northeastern University at Qinhuangdao, School of Computer and Communication Engineering, Qinhuangdao, Hebei, 066004, China

* Corresponding Author Email: 19846733685@163.com

Abstract. Parkinson's disease (Parkinson's disease, PD) is a common neurodegenerative disorder of the nervous system. Beyond severely compromising patients' quality of daily life, it also induces non-motor symptoms such as cognitive impairment and depression, thereby imposing a heavy burden on patients' families and society as a whole. Conventional PD detection methods, however, are constrained by their dependence on manual feature extraction and susceptibility to noisy data. These methods suffer from limitations including relatively low detection accuracy and insufficient feature extraction capability, making them barely able to meet the requirements for precision and stability in clinical diagnosis.To address the limitations of conventional methods, this study proposes a Deep Residual Shrinking Network (Deep Residual Shrinking Network, DRSN) based on pooling fusion for efficient detection of Parkinson's disease. First, by introducing residual connections into the network structure, the risks of gradient vanishing or gradient exploding caused by excessive network depth are effectively mitigated, ensuring the effective learning of deep-level features. Second, a multi-scale pooling feature fusion strategy is adopted to extract richer local features from Electroencephalogram (Electroencephalogram, EEG) signals. Meanwhile, an attention mechanism is integrated to automatically derive the optimal threshold of the soft-thresholding function, enabling adaptive removal of noise in the signals and enhancing the representational capability of effective features.The proposed method was validated on the Parkinson's disease neurophysiological activity dataset and the New Mexico dataset. The results demonstrate that the DRSN method achieved an accuracy of 92.10%, precision of 91.27%, recall of 90.72%, and F1-score of 90.99% on the PD neurophysiological activity dataset. On the New Mexico dataset, it further yielded an accuracy of 98.15%, precision of 97.63%, recall of 96.12%, and F1-score of 96.87%. In comparison with traditional methods—including convolutional neural networks (accuracy: 88.00%) and deep residual networks (accuracy: 92.03%)—the proposed method exhibited an accuracy improvement of 10.15 percentage points and 6.12 percentage points, respectively.Leveraging the residual connections that ensure the stability of deep networks, the multi-scale pooling fusion that enables the extraction of rich features, and the attention mechanism-driven adaptive denoising capability, this method demonstrates distinct advantages in Parkinson's disease detection. It effectively enhances detection accuracy and robustness, thereby providing more reliable technical support for the auxiliary diagnosis of Parkinson's disease.

Keywords: Parkinson's Disease; Pooling Fusion; DRSN; Noise Resistance; Detection Accuracy.

1. Introduction

Parkinson's disease (PD) is a prevalent age-related neurodegenerative disorder in the elderly population, frequently accompanied by a spectrum of non-motor symptoms such as constipation, hyposmia, insomnia, emotional disturbances, and cognitive decline. This disease exerts a profound adverse impact on the quality of life of both patients and their families [1]. Currently, there are over 5 million people living with PD in China, accounting for 43.14% of the global PD patient population. Owing to the high heterogeneity of PD, patients exhibit substantial variability in multiple dimensions, including age at onset, clinical manifestations, therapeutic responses, and disease progression rate. Therefore, the early achievement of disease detection, prediction of disease progression, and accurate patient classification is of pivotal importance for the implementation of precision medicine. Against this backdrop, the adoption of efficient detection approaches holds significant implications for advancing PD clinical management.

Traditional detection modalities for Parkinson's disease (PD) include clinical symptom assessment [2], dopamine transporter (DAT) imaging [3], and neuroimaging examinations [4]—such as computed tomography (CT) and magnetic resonance imaging (MRI). Clinical symptom assessment relies on the observation of patients' typical motor symptoms, including resting tremor, muscle rigidity, bradykinesia, and postural balance impairment, with diagnostic judgments made by integrating the presence and severity of these symptoms. Nevertheless, this method is highly subjective: it is prone to misdiagnosis when early-stage symptoms are atypical, which imposes inherent limitations on its diagnostic accuracy. DAT imaging enables the visualization of the functional status of dopaminergic neuron terminals via positron emission tomography-computed tomography (PET-CT) following the injection of radioactive tracers, and it aids in diagnosis based on the reduced tracer uptake in the striatal region. However, this technique is encumbered by notable drawbacks: it incurs substantial costs, requires radioactive pharmaceuticals, imposes strict demands on equipment and resource allocation, and exhibits a combined false-positive and false-negative rate of approximately 5%. CT and MRI are employed to rule out PD-like symptoms caused by other organic diseases through anatomical imaging. Yet, they lack specific manifestations for PD itself and are ineffective in detecting subtle early-stage pathological changes. Specifically, CT exposes patients to ionizing radiation; MRI, by contrast, is time-consuming and costly, and it is contraindicated for patients with certain intracorporeal metal implants (e.g., pacemakers, deep brain stimulation electrodes). In contrast, electroencephalogram (EEG) signal detection—an approach that explores PD pathogenesis by analyzing abnormal brain wave patterns in affected patients—offers distinct and compelling advantages. Compared with clinical symptom assessment, it demonstrates greater objectivity by minimizing inter-rater variability. Unlike DAT imaging, it eliminates the need for radioactive substances, thereby enhancing safety and reducing associated costs. Furthermore, EEG is more sensitive to fluctuations in cerebral functional activity, enabling the capture of subtle early-stage neurophysiological alterations—an attribute that outperforms CT and MRI, as the latter two show no specific imaging changes in early PD and are burdened by high equipment and examination expenses.

Göker et al. calculated the Power Spectral Density (PSD) of EEG signals across the frequency range of 1 to 49 Hz using periodogram, Welch, and multitaper spectral analysis methods, respectively. This approach achieved a specificity of 0.965, a sensitivity of 0.994, a precision of 0.964, and an accuracy of 97.92% [5]. Nevertheless, PSD primarily reflects the power distribution of signals across different frequencies; its capacity to capture the subtle, complex changes in EEG signals that occur during the early stages of PD is limited, making it difficult to accurately identify ambiguous and atypical features. Zhang et al. quantified the synchrony of EEG channels across different frequency bands (delta, theta, alpha, and beta) in early PD by calculating the phase synchronization index. By comparing the graph-theoretic features in the delta band between the PD group and the healthy control (HC) group, the study concluded that there are significant differences in specific frequency bands of brain network structure between patients with early PD and healthy subjects, with patients with early PD exhibiting abnormal characteristic brain activity in specific frequency bands [6]. However, the frequency band analysis scope of this method is relatively narrow: it only focuses on comparing the graph-theoretic features of the delta band and fails to fully incorporate the analysis of synchrony differences across other frequency bands. Minh Tai Pham Nguyen et al. proposed Dense Multiscale Sample Entropy (DM-SamEn), which adopts a weighting mechanism to reduce redundancy. In PD classification, this method achieved a maximum accuracy of 98.38% [7]. That said, this method relies on reliable and publicly accessible datasets for its data source, which may lead to data imbalance; additionally, it exhibits excessive dependence on a single dataset. B. Vidya et al. developed a gait classification-based decision support system using a Multiclass Support Vector Machine (MCSVM), employing a multiple regression method to normalize gait time-series data. Experimental results demonstrated that the quadratic SVM achieved an average accuracy of 98.65%, outperforming several other state-of-the-art methods that utilize gait datasets for PD diagnosis [8]. However, this method integrates multiple binary classifiers through "one-vs-one" or "one-vs-rest" strategies, which significantly increases the complexity of the model. In recent years, deep learning-based methods

have been increasingly applied in PD detection, including Convolutional Neural Networks (CNNs), Long Short-Term Memory (LSTM) networks, Graph Convolutional Networks (GCNs), and Deep Residual Networks (ResNets).

Sivaranjini S et al. refined the diagnosis of Parkinson's disease (PD) using the AlexNet architecture, a type of Convolutional Neural Network (CNN). They trained magnetic resonance (MR) images through a transfer learning network and conducted tests to measure diagnostic accuracy, achieving an accuracy rate of 88.9% [9]. However, due to the relatively shallow depth of the AlexNet model, its ability to capture subtle structural changes related to PD in MR images is limited, which may result in the omission of key pathological features. Fatih Demir et al. transformed all input feature vectors into input images and employed a deep Long Short-Term Memory (LSTM) network for PD diagnosis, attaining an accuracy of 94.27% [10]. Nevertheless, the process of converting feature vectors to images in this method lacks clear medical justification. If unreasonable approaches are adopted for dimension mapping, pixel assignment, or other conversion steps, the inherent correlations between original features may be disrupted and lost. Utsha Saha et al. proposed a diagnostic approach combining Graph Convolutional Networks (GCNs) with an Euclidean distance-based graph construction method. This method learns meaningful feature representations from graph-structured data while capturing similarities between patient samples, ultimately achieving a high classification accuracy of 97.4% on the test set [11]. However, this method has a limitation in graph construction: it solely relies on Euclidean distance to measure similarities between patient samples. In clinical practice, however, the pathological features of patients often exhibit non-linear correlations, and clinical similarities do not necessarily conform to the linear assumptions of Euclidean space—this restricts the model's ability to characterize complex pathological features to a certain extent. Lucas de O. Santos et al. utilized a Residual Neural Network for PD diagnosis, following a specific workflow: first converting Electroencephalogram (EEG) signals to the frequency domain, identifying spectral markers via directed graphs, integrating multi-channel data, and finally classifying the generated spectral tensors using different neural network architectures. This method yielded an accuracy of 96.7%, a precision of 97.22%, and an F1-Score of 96.63% [12]. Yet, it has a notable drawback: the frequency-domain transformation leads to the loss of time-domain information. EEG signals contain rich temporal dynamic features, and simply converting them to the frequency domain for analysis tends to overlook transient waveform changes. This impairs the accuracy of capturing sudden neural activities and is unfavorable for excavating subtle neurophysiological features associated with early-stage PD.

In view of the limitations of the aforementioned methods, this study proposes the use of a Deep Residual Shrinking Network (DRSN) based on pooling fusion for PD detection. During the threshold derivation stage of the Deep Residual Shrinking Network, this method employs both average pooling and max pooling to simultaneously extract multi-scale features of EEG signals and perform feature fusion, thereby further enhancing its diagnostic accuracy in real-world scenarios. Experiments have demonstrated that the DRSN-PF method proposed in this study can effectively achieve disease diagnosis under noise conditions with different Signal-to-Noise Ratios (SNR).

2. Datasets

2.1 Neurophysiological Activity Datasets for Parkinson's Disease

This dataset encompasses Electroencephalogram (EEG) signals that are modeled to simulate neural activity in patients with Parkinson's Disease. It is designed to underpin research in biomedical signal processing, as well as investigations into machine learning models tailored for the analysis and modulation of neural activity. The salient features of this dataset are outlined as follows: First, it contains raw time-series EEG signals with artificially introduced noise, which serves to replicate neural activity in real-world scenarios. Second, time-frequency features are derived through the application of the Short-Time Fourier Transform (STFT)—a technique employed to extract magnitude and phase components, thereby enabling meticulous time-frequency domain analysis.

Third, it incorporates metadata that includes patient-specific information such as age, gender, clinical stage, and condition labels, facilitating contextual comprehension of the data. Fourth, a target column is included, where numerical labels correspond to distinct states of Parkinson's Disease: specifically, 0 denotes Rest Tremor, 1 represents Rigidity, 2 indicates the Normal state, and 3 stands for the On-Medication state. In essence, this dataset comprises synthetic EEG signal data simulated for Parkinson's Disease research, encompassing four core components: patient metadata (including attributes such as age, gender, clinical stage, and condition labels); raw neural signals augmented with noise to mimic real-world environments; STFT-derived features (encompassing magnitude and phase components extracted via STFT); and numerical classifications corresponding to Parkinson's Disease states (e.g., Rest Tremor, Rigidity, Normal state, and On-Medication state). The dataset is accessible at the following link: https://www.kaggle.com/datasets/ziya07/neural-activity-dataset-for-parkinsons-disease

2.2 The New Mexico Dataset

This dataset was collected by the University of New Mexico (UNM) and comprises electroencephalogram (EEG) signal data from 27 patients with Parkinson's Disease (PD) and 27 gender-matched healthy controls. The PD patients visited the laboratory twice for data collection, with an interval of 7 days [13]: one visit occurred during the period when they were on medication, and the other took place after an overnight withdrawal from medication for 15 hours. Consequently, this dataset contains information on the 27 PD patients in both treated (on-medication) and untreated (off-medication) states.For each patient and control subject, data were collected over a duration of two minutes. The EEG data were acquired at a sampling rate of 500 Hz using 64 silver/silver chloride (Ag/AgCl) channels, with an online reference to the CPz electrode and via the Brain Vision data acquisition system. As a result, CPz channel data are absent from this dataset.

3. Methodology

3.1 Theoretical Foundations

The Deep Residual Shrinkage Network (DRSN) can be regarded as a variant of the Convolutional Neural Network (CNN). It retains the core architecture of CNN while integrating residual learning, soft-threshold denoising, and the Attention Mechanism (AM). This integration approach not only effectively addresses the challenge of training traditional deep networks— a long-standing issue in deep learning—but also enhances the feature extraction performance for noisy vibration signals, thereby endowing the network with excellent denoising capability.

3.1.1 Residual Learning

The ideology of residual learning, leveraging its unique identity mapping structure, has been widely adopted in deep learning architectures. This structure can effectively mitigate the phenomena of gradient vanishing or gradient exploding that often occur in deep network architectures. The specific structure is illustrated in Figure 1. Residual learning can be mathematically expressed as formulated as Equation (1):

$$Y = \Gamma\left(X, S_i\right) + X \tag{1}$$

In the formula(1): X and Y denote the input vector and output vector, respectively; S_i represents the coefficient of the i-th weight layer; and Γ stands for the residual function, whose expression is given by:

$$\Gamma = \mathbf{S}_2 \gamma\left(\mathbf{S}_1^T X\right) \tag{2}$$

In Equation(2), γ denotes the activation function.

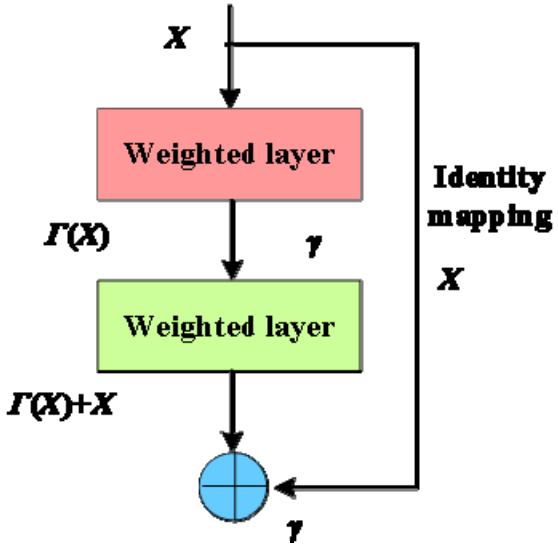

Figure 1. Structure of Residual Learning

3.1.2 Soft-Thresholding Function

The soft-thresholding function is a widely employed denoising function, whose core idea lies in eliminating near-zero features within the threshold region. The definition of the soft-thresholding function is given by:

$$y = f(x) = \begin{cases} sgn(x)(|x| - \tau), & |x| \geq \tau; \\ 0, & |x| < \tau. \end{cases} \tag{3}$$

In Formula (3): x and y represent the input feature and output feature, respectively; τ denotes the threshold; $sgn(\cdot)$ is a sign function. When $x > 0$, $sgn(x) = 1$; when $x = 0$, $sgn(x) = 0$; when $x < 0$, $sgn(x) = -1$.

Threshold setting is a crucial issue in soft - threshold denoising. In Reference [14], the sum of squares is first calculated for the coefficient T. Then, within the window centered on wavelet coefficients, the corresponding shrinkage factor θ is computed, and thus the global threshold is obtained. Based on this, it is determined whether the wavelet coefficients should undergo shrinkage towards θ or be directly set to θ.

3.1.3 Attention Mechanism

Squeeze-and-Excitation (SE), a commonly used attention mechanism, enables adaptive adjustment of the network's degree of focus on feature information across different channels. It can be employed to emphasize critical features while de-emphasizing irrelevant ones [15]. The workflow of the SE mechanism proceeds as follows: first, these features are compressed into a channel descriptor to obtain aggregated features that encapsulate global information. For this compression process, the calculation formula for the i-th element of the aggregated features is given by:

$$y_i = \frac{1}{a \times b} \sum_{m=1}^{a} \sum_{n=1}^{b} x_i(m,n) \tag{4}$$

In Formula(4), $a \times b$ represents the spatial dimension.

The weight coefficients s of different channels are obtained through the excitation step, and the calculation method is as follows:

$$s = \sigma\left(W_2 \delta\left(W_1 y\right)\right) \tag{5}$$

In Formula(5): σ and δ denote the Sigmoid and ReLU activation functions, respectively, and W_i represents the i-th set of trainable parameters.

3.2 DRSN Based on Pooling Fusion

3.2.1 The DRSN Network

As illustrated in Figure 2, the Deep Residual Shrinkage Network (DRSN) comprises an input layer, convolutional layers (Conv), residual shrinkage building units (RSBU), batch normalization layers (BN), rectified linear unit layers (ReLU), a global average pooling layer (GAP), fully connected layers (FC), and an output layer [16].

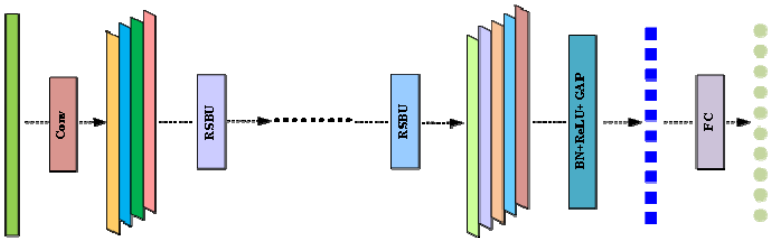

Figure 2. Overall Architecture of the DRSN

Convolutional layers (Conv) are a key component that distinguishes them from traditional fully connected neural networks. They are implemented using convolution instead of matrix multiplication, which enables the convolution kernels in the convolutional layer to have fewer parameters than the transformation matrices in fully connected layers (FC).

Batch normalization (BN) is a feature normalization technique. It is inserted into deep learning architectures as a trainable process, aiming to transform features into an ideal distribution, thereby accelerating the training speed.

The rectified linear unit (ReLU) is one of the most popular activation functions in deep neural networks. The partial derivative of its non-zero output feature with respect to the input feature is always 1, which can effectively reduce the risk of gradient explosion and vanishing.

Global average pooling (GAP) calculates the average value of each channel of the output feature map, thereby reducing the number of parameters that need to be trained in the fully connected layer (FC).

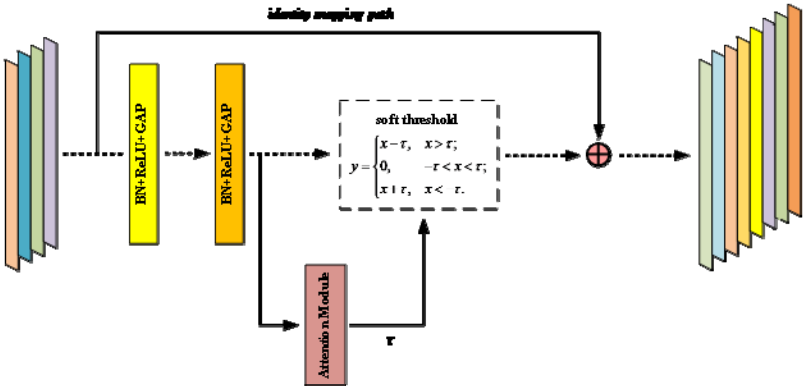

Figure 3. Overall Architecture of the RSBU

As the core module of the DRSN, the residual shrinkage building unit (RSBU) integrates basic functional components in its structural design and innovatively incorporates the idea of residual learning and the soft-thresholding denoising mechanism, as shown in Figure 3. Specifically, on the one hand, an efficient gradient conduction channel is built through the identity mapping path to ensure that gradients can effectively flow to the shallow network close to the input layer, thereby significantly improving the parameter update efficiency and reducing the training difficulty. On the other hand, an attention mechanism is used to adaptively derive the corresponding threshold for each sample, and then the soft-thresholding function is used to achieve accurate denoising of vibration signals, and the specific process is shown in Figure 4. Based on the above modular design innovations,

compared with traditional CNNs, DRSN not only has significant advantages such as lower training difficulty and stronger denoising ability but has also been widely used in the field of fault diagnosis.

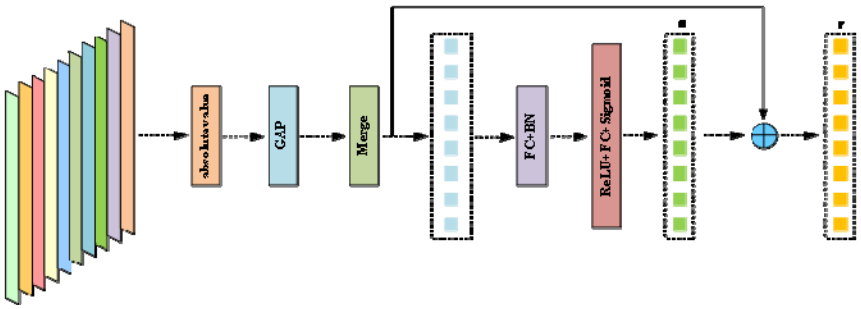

Figure 4. Structure of the Attention Module

3.2.2 DRSN Based on Pooling Fusion

As illustrated in Figure 5, the Deep Residual Shrinkage Network based on Pooling Fusion (DRSN-PF), innovatively proposed in this study, adopts a multi-pooling fusion structure where the max-pooling layer and average-pooling layer work in synergy, replacing the Global Average Pooling (GAP) in the original model. This design is not a simple component replacement, but rather achieves information gain in the threshold derivation stage through the complementary characteristics of the two pooling methods: max-pooling excels at capturing the extreme value information of salient features, while average-pooling can preserve the overall trend of feature distribution. The fusion of the two enables the thresholds generated by the attention module to more comprehensively cover the diverse attributes of local features. This information compensation mechanism directly enhances the model's ability to extract weak features from noisy vibration signals. The remaining architectural components of DRSN-PF remain consistent with the original DRSN, ensuring the pertinence of the innovative design and the stability of the system.

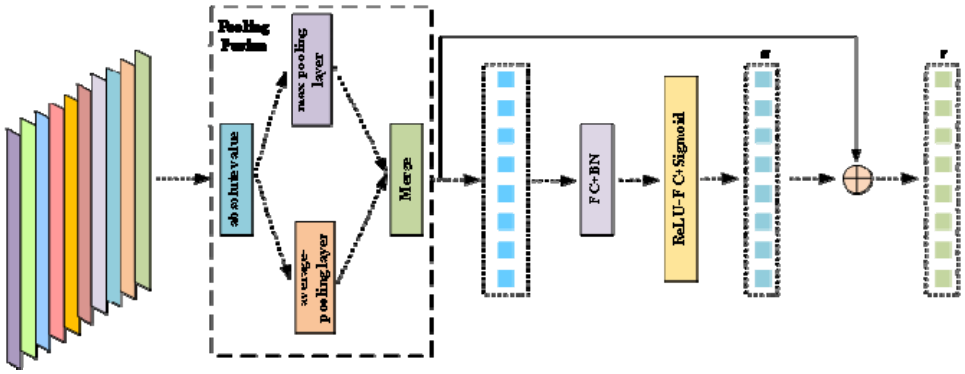

Figure 5. Structure of the Attention Module Based on Pooling Fusion

4. Dataset

4.1 Detection Results of Neural Activity Datasets for PD

For the EEG dataset of Parkinson's disease (PD) in question, the preprocessing and feature engineering procedures were implemented as follows: First, age, a continuous variable in the metadata, was subjected to normalization to eliminate the influence of different magnitude scales. In contrast, categorical variables—including gender and clinical stage—were encoded using one-hot encoding, a standard technique to convert discrete categorical information into a numerical format compatible with machine learning models. Second, regarding the raw EEG signals contaminated with simulated noise, a band-pass filter (0.5–40 Hz) was applied. This filtering step aimed to retain the primary frequency bands associated with neural activity (e.g., delta, theta, alpha, beta, and low gamma

bands) while suppressing extraneous noise components outside this range. Subsequent to filtering, the EEG signals were segmented into fixed-length epochs and standardized (i.e., z-score normalization) to ensure that each signal channel had a mean of 0 and a standard deviation of 1, mitigating the impact of inter-channel amplitude variations. Third, for the existing time-frequency features derived from Short-Time Fourier Transform (STFT)—encompassing both amplitude and phase components—dimensionality reduction was performed. This was achieved through either feature selection (to retain only the most discriminative features) or Principal Component Analysis (PCA, to transform the feature space into a lower-dimensional subspace while preserving the majority of variance), thereby alleviating the curse of dimensionality and improving computational efficiency. Fourth, the processed metadata features (normalized age and one-hot encoded categorical variables), filtered EEG time-domain features, and dimensionally reduced STFT time-frequency features were effectively fused and aligned. This fusion step ensured temporal and semantic consistency across different feature modalities, integrating complementary information from demographic, raw signal, and time-frequency domains. Finally, to address the class imbalance issue inherent in the classification labels (a common challenge in medical datasets), techniques such as oversampling (e.g., Synthetic Minority Oversampling Technique, SMOTE) were employed to balance the sample distribution across different classes. Through the aforementioned steps, a unified and well-structured feature matrix was constructed for subsequent model training and validation. The dataset was split into a training set and a test set at a ratio of 7:3. The detailed performance metrics of dataset validation are presented in Table 1.

Table 1. Dataset Validation Results

Evaluation Metric	Accuracy	Precision	Recall	F1 Score
Value (%)	92.10	91.27	90.72	90.99

As can be seen from Table 1, the detection results of DRSN on the Parkinson's disease neural activity dataset show that the accuracy is 92.10%, the precision is 91.27%, the recall is 90.72%, and the F1 score is 90.99%. An accuracy of 92.10% verifies the efficient discrimination ability of the multi-feature fusion architecture for the four types of labels, namely "resting tremor", "rigidity", "normal", and "medication state", and solves the problems of insufficient feature extraction and weak noise resistance of traditional methods. A precision of 91.27% reduces false-positive misjudgments. A recall of 90.72% reduces the risk of early missed diagnosis, and an F1 score of 90.99% achieves a balance between "precision" and "comprehensiveness".

4.2 Detection Results of the New Mexico Dataset

For the University of New Mexico (UNM) Parkinson’s disease (PD) EEG dataset, the preprocessing workflow was implemented in the following sequential steps: First, **channel-level operations** were performed. Owing to the absence of CPz channel data—a consequence of using an online CPz reference during data acquisition—an alternative valid electrode configuration was adopted for re-referencing, specifically converting to a whole-brain average reference to ensure spatial consistency of the EEG signals across all channels. Second, the raw EEG signals, originally sampled at 500 Hz, were downsampled to 250 Hz. This step aimed to reduce redundant data volume while preserving critical neural activity information. Concurrently, a band-pass filter (e.g., 0.5–45 Hz) was applied to eliminate low-frequency drifts (attributed to physiological artifacts such as respiration or skin potential) and high-frequency noise (e.g., electromagnetic interference), thereby refining the signal-to-noise ratio. Third, **artifact removal** was conducted via Independent Component Analysis (ICA). This technique enabled the identification and subsequent removal of non-neural biological artifacts, including electrooculographic (EOG) signals (resulting from eye movements or blinks) and electromyographic (EMG) signals (originating from muscle tension), which could otherwise confound the interpretation of neural activity. Fourth, the continuous two-minute EEG recordings were segmented into equal-length epochs based on experimental conditions (e.g., resting state or task-

specific periods). Baseline correction was further applied to each epoch to adjust for signal offsets relative to a pre-defined baseline period, ensuring that variations in signal amplitude reflected true neural fluctuations rather than baseline drifts. Fifth, data normalization was performed on recordings corresponding to different states (medicated vs. unmedicated) for each participant. This step standardized the signal amplitude scale across all conditions, eliminating potential biases arising from inter-state differences in signal magnitude and facilitating cross-condition comparisons. Finally, a labeled dataset was constructed, encompassing data from both PD patients and healthy control subjects, as well as from PD patients in distinct medication states (medicated vs. unmedicated). This preprocessed and labeled dataset laid the foundation for subsequent feature extraction and analysis across the time domain, frequency domain, and time-frequency domain. The validation results of this dataset are presented in Table 2.

Table 2. Dataset Validation Results

Evaluation Metric	Accuracy	Precision	Recall	F1 Score
Value (%)	98.15	97.63	96.12	96.87

As indicated in Table 2, the model constructed by DRSN demonstrates exceptional performance in detection tasks using the UNM Parkinson's disease (PD) EEG dataset. Specifically, it achieves an accuracy of 98.15%, a precision of 97.63%, a recall of 96.12%, and an F1 score of 96.87%—all metrics attaining notably high levels. These results underscore that the model exhibits three key strengths in classification tasks: strong overall accuracy in distinguishing between classes, robust capability to correctly identify positive cases (e.g., PD-related states), and a well-balanced trade-off between recall (capturing true positive cases) and precision (minimizing false positive cases).

5. Discussion

5.1 Comparison with Alternative Methods

To demonstrate the advantages of the pooling fusion-based DRSN proposed in this study for Parkinson's disease (PD) detection, a comparative analysis was conducted against traditional PD detection methods. Specifically, the accuracy of conventional approaches—including Convolutional Neural Network (CNN), Multi-Scale Convolutional Neural Network (MSCNN), Long Short-Term Memory (LSTM), Deep Residual Networks (ResNet), and Transformer—was evaluated on the same neural activity dataset of PD. The comparative results are presented in Table 3.

Table 3. Comparison of Accuracy Among Various Methods on the Parkinson's Disease Neural Activity Dataset

Reference	Method	Accuracy (%)
[17]	CNN	88%
[18]	LSTM	83%
[19]	MCNN	85.87
[20]	ResNet	92.03%
[21]	Transformer	83.3%
This work	DRSN	92.10

As shown in Table 3, on the Parkinson's disease (PD) neural activity dataset, the DRSN method proposed in this study achieves an accuracy of 92.10%, demonstrating significant advantages over traditional deep learning approaches. Specifically, the accuracy of DRSN outperforms that of CNN (88%), LSTM (83%), MSCNN (85.87%), and Transformer (83.3%). Even when compared with ResNet (92.03%)—another method that also leverages the advantages of deep network architectures—the marginal improvement in accuracy still reflects DRSN's optimized performance in feature extraction and noise suppression.This superiority can be attributed to three core design features of DRSN: first, residual connections ensure the stability of deep network training, mitigating

the vanishing gradient problem common in deep models; second, attention mechanism-driven adaptive denoising effectively filters out irrelevant noise from EEG signals; and third, multi-scale pooling fusion enhances the representation of critical discriminative features. Together, these components address the inherent limitations of traditional methods—such as insufficient feature capture in noisy EEG signals and weak anti-interference capability—thereby further validating that DRSN outperforms existing mainstream deep learning models in PD detection tasks.

Table 4. Comparison of Accuracy Among Various Methods on the UNM Dataset

Reference	Method	Accuracy(%)
[22]	MCPNet	92.5%
[23]	CNN-BiLSTM	97.24%
[24]	GNN	69.40%
[25]	CNN	93.10%
[26]	transformer	94%
This work	DRSN	98.15

As indicated in Table 4, on the UNM Parkinson's disease (PD) EEG dataset, the DRSN method proposed in this study achieves an accuracy of 98.15%, which significantly outperforms other comparative methods, demonstrating robust classification performance and strong environmental adaptability. Specifically, the accuracy of DRSN not only far surpasses that of models with inherent limitations in graph-structured data processing—such as Graph Neural Network (GNN), which yields an accuracy of 69.40—but also exceeds that of methods optimized for EEG signal analysis, including traditional Convolutional Neural Network (CNN, 93.10%), Transformer (94%), and MCPNet (92.5%). Even when compared with the relatively high-performance CNN-BiLSTM (97.24%), DRSN still achieves an improvement of nearly 1 percentage point.The core driver of this superiority lies in the unique characteristics of the UNM dataset: it includes data from PD patients in both medicated and unmedicated states as well as from healthy controls, while also suffering from missing data in the CPz channel. In response to these challenges, DRSN leverages a pooling fusion strategy to fully integrate global distribution information and local extreme value information of features. Complemented by an attention mechanism that adaptively enhances features from key channels, DRSN effectively mitigates interference caused by data incompleteness and state variability. Meanwhile, its residual shrinkage structure suppresses the impact of noise on feature extraction. Collectively, these design elements enable DRSN to achieve more stable and accurate PD detection results than existing mainstream models in complex data scenarios.

5.2 Research Limitations and Future Improvement Directions

Despite the superior performance of DRSN on the New Mexico dataset and the Parkinson's disease (PD) neural activity dataset, the current study has a notable limitation: it focuses solely on the association between neuroelectric activity features and disease states, without delving into the dynamic relationship between these features and disease progression.

In future research, longitudinal follow-up data could be integrated to construct a "feature-disease progression" prediction model. This enhancement would enable DRSN to not only achieve accurate PD detection but also provide support for evaluating disease progression—thereby further expanding its clinical application value.

6. Conclusion

To address the early detection and classification of Parkinson's disease (PD), this study proposes a DRSN method based on pooling fusion. By integrating average pooling and max pooling strategies, this method exhibits significant advantages in multi-scale feature extraction and noise suppression, effectively enhancing the model's classification performance in real-world noisy environments. Experimental results on the PD neural activity dataset and the UNM PD EEG dataset demonstrate

that DRSN achieves an accuracy of 92.10% and 98.15%, respectively. Meanwhile, its precision, recall, and F1 score all remain at relatively high levels—these outcomes validate that the model possesses excellent classification consistency, robustness, and generalization capability across datasets of different origins and under varying signal-to-noise ratio (SNR) conditions. This study not only provides a new and effective tool for the auxiliary diagnosis of PD but also offers a referable deep learning model design framework for the detection of neurological diseases based on EEG signals. Consequently, it holds considerable potential for clinical translation and high application value.

References

[1] Clarke C E. Parkinson's disease[J]. Bmj, 2007, 335(7617): 441-445.

[2] Jankovic J. Parkinson’s disease: clinical features and diagnosis[J]. Journal of neurology, neurosurgery & psychiatry, 2008, 79(4): 368-376.

[3] Akdemir Ü Ö, Bora H A T, Atay L Ö. Dopamine transporter spect imaging in Parkinson's disease and parkinsoniandisorders[J]. Turkish journal of medical sciences, 2021, 51(2): 400-410.

[4] Brooks D J, Frey K A, Marek K L, et al. Assessment of neuroimaging techniques as biomarkers of the progression of Parkinson's disease[J]. Experimental neurology, 2003, 184: 68-79.

[5] Göker H. Automatic detection of Parkinson’s disease from power spectral density of electroencephalography (EEG) signals using deep learning model[J]. Physical and engineering sciences in medicine, 2023, 46(3): 1163-1174.

[6] Zhang W, Han X, Qiu S, et al. Analysis of brain functional network based on EEG signals for early-stage Parkinson’s disease detection[J]. IEEE Access, 2022, 10: 21347-21358.

[7] Nguyen M T P, Tran M K P, Nakano T, et al. An approach for detecting Parkinson’s disease by integrating optimal feature selection strategies with dense multiscale sample entropy[J]. Information, 2024, 16(1): 1.

[8] Vidya B, Sasikumar P. Gait based Parkinson’s disease diagnosis and severity rating using multi-class support vector machine[J]. Applied Soft Computing, 2021, 113: 107939.

[9] Sivaranjini S, Sujatha C M. Deep learning based diagnosis of Parkinson’s disease using convolutional neural network[J]. Multimedia tools and applications, 2020, 79(21): 15467-15479.

[10] Demir F, Sengur A, Ari A, et al. Feature mapping and deep long short term memory network-based efficient approach for Parkinson’s disease diagnosis[J]. IEEE Access, 2021, 9: 149456-149464.

[11] Saha U, Ahamed I U, Ahamed I U, et al. Graph convolutional network-based approach for parkinson’s disease classification using euclidean distance graphs[C]//2024 7th International Conference on Informatics and Computational Sciences (ICICoS). IEEE, 2024: 532-537.

[12] Santos L O, Medeiros A G, Rego P A L, et al. Graph-Based EEG Analysis for Parkinson’s Disease Classification: A Residual Neural Network Approach[C]//2024 International Joint Conference on Neural Networks (IJCNN). IEEE, 2024: 1-8.

[13] Chauhan M K, Ghosal P. A Hybrid CNN-BiLSTM Neural Network Architecture for Early Prediction of Parkinson's Disease[C]//2024 IEEE International Symposium on Smart Electronic Systems (iSES). IEEE, 2024: 303-308.

[14] Dai Y, Tang Z, Wang Y, et al. Data driven intelligent diagnostics for Parkinson’s disease[J]. Ieee Access, 2019, 7: 106941-106950.

[15] Mekruksavanich S, Jitpattanakul A. Detection of freezing of gait in parkinson's disease by squeeze-and-excitation convolutional neural network with wearable sensors[C]//2021 15th International Conference on Open Source Systems and Technologies (ICOSST). IEEE, 2021: 1-5.

[16] Zhao M, Zhong S, Fu X, et al. Deep residual shrinkage networks for fault diagnosis[J]. IEEE Transactions on Industrial Informatics, 2019, 16(7): 4681-4690.

[17] Khatamino P, Cantürk I, Özyılmaz L. A deep learning-CNN based system for medical diagnosis: An application on Parkinson’s disease handwriting drawings[C]//2018 6th international conference on control engineering & information technology (CEIT). IEEE, 2018: 1-6.

[18] Reyes J F, Montealegre J S, Castano Y J, et al. LSTM and Convolution Networks exploration for Parkinson's Diagnosis[C]//2019 IEEE Colombian Conference on Communications and Computing (COLCOM). IEEE, 2019: 1-4.

[19] Qiu L, Li J, Pan J. Parkinson's disease detection based on multi-pattern analysis and multi-scale convolutional neural networks[J]. Frontiers in Neuroscience, 2022, 16: 957181.

[20] Yang X, Ye Q, Cai G, et al. PD-ResNet for classification of Parkinson's disease from gait[J]. IEEE Journal of Translational Engineering in Health and Medicine, 2022, 10: 1-11.

[21] Güven M. Detection of Alzheimer's and Parkinson's diseases using deep learning-based various transformers models[J]. Engineering Proceedings, 2024, 73(1): 4.

[22] Qiu L, Li J, Zhong L, et al. A novel EEG-based Parkinson's disease detection model using multiscale convolutional prototype networks[J]. IEEE Transactions on Instrumentation and Measurement, 2024, 73: 1-14.

[23] Chauhan M K, Ghosal P. A Hybrid CNN-BiLSTM Neural Network Architecture for Early Prediction of Parkinson's Disease[C]//2024 IEEE International Symposium on Smart Electronic Systems (iSES). IEEE, 2024: 303-308.

[24] Neves C, Zeng Y, Xiao Y. Parkinson's disease detection from resting state EEG using multi-head graph structure learning with gradient weighted graph attention explanations[C]//International Workshop on Machine Learning in Clinical Neuroimaging. Cham: Springer Nature Switzerland, 2024: 3-12.

[25] Rizvi S Q A, Wang G, Khan A, et al. Classifying Parkinson's disease using resting state electroencephalogram signals and U EN-PDNet[J]. IEEE access, 2023, 11: 107703-107724.

[26] Afonso M M, Edla D R, Ramesh D. Transformers-Based Deep Learning for Parkinson's Disease Detection Using Electroencephalography and Stockwell Transform[J]. Procedia Computer Science, 2025, 258: 4094-4104.